Influence of electronic stopping on sputtering induced by cluster impact on metallic targets

Luis Sandoval and Herbert M. Urbassek*
Fachbereich Physik und Forschungszentrum OPTIMAS, Universität Kaiserslautern, Erwin-Schrödinger-Straße, D-67663 Kaiserslautern, Germany

(Received 12 January 2009; revised manuscript received 15 March 2009; published 23 April 2009)

Using molecular-dynamics simulation, we model the sputtering of a Au (111) crystallite induced by the impact of Au_{13} projectiles with total energies up to 500 keV. Due to the uncertainty of the electronic stopping of Au moving in particular at small velocities, we performed several simulations, in which the electronic stopping parameters are systematically changed. Our results demonstrate the dominating influence of the cut-off energy E_c, below which the high-velocity electronic stopping of atoms is switched off in the simulation. If E_c is smaller than roughly one half the cohesive energy of the target, sputtering ceases after a few ps; the spike contribution to sputtering (also called phase explosion or gas-flow contribution) is entirely quenched and the sputtering yield is up to an order of magnitude smaller than when electronic stopping is taken into account only at higher atom energies. Our results demonstrate the importance of a careful modeling of electronic stopping in simulations of spike sputtering from metals.

DOI: 10.1103/PhysRevB.79.144115 PACS number(s): 79.20.Rf, 79.20.Ap, 61.80.Lj, 34.50.Bw

I. INTRODUCTION

Energetic projectiles impinging on solid targets may lead to the sputtering of atoms and clusters from the solid surface.[1,2] Basically, two mechanisms have been identified to be responsible for the sputtering. (i) The *collision cascade*: the projectile conveys its energy in a series of collisions to target atoms; these recoil with further atoms, etc., and thus the so-called collision cascade has been generated. Atoms from (near to) the target surface, which recoil in the collision cascade, may become sputtered if their energy is larger than the cohesive energy, E_{coh}, of the solid. This mechanism is responsible for sputtering in many projectile-target systems and is well understood. It is fast (of the order of 1 ps or faster), since after this time recoil energies have become too small to overcome the surface binding energy. (ii) The *spike*: the collision cascade described above may become dense[3] in the sense that moving particles collide with each other. If the energy density in a surface volume (called the spike volume) becomes sufficiently large—roughly of the order of the cohesive energy per atom or the critical temperature of the liquid-gas phase transition–, the interatomic bonding is weakened and a collective flow of the spike volume out of the target may start, leading to abundant sputtering. This mechanism has also been termed *gas flow* or *phase explosion* mechanism. It may be operative when high energy densities are deposited—and thus for heavy projectiles and in particular for cluster impact—and also for targets with small cohesive energies (such as condensed-gas targets). In these cases, it has been found to be operative after an early collision-cascade phase; depending on the system, the spike may last several ten ps or even >100 ps.

Besides colliding with other atoms (nuclear stopping), moving atoms may also give part of their energy to target electrons. In an often adopted scheme due to Lindhard and Scharff[4] (LS) the stopping force (energy loss per path length traveled) is taken to be proportional to the atom velocity v. In collision-cascade theory, the effect of electronic stopping on sputtering is easily taken into account. Since only atoms with a kinetic energy exceeding the cohesive energy can be sputtered, atom trajectories are only followed down to a minimum kinetic energy of $E_{kin}=E_{coh}$. Since collision-cascade sputtering ceases after a few 100 fs as a rule, electronic stopping influences the sputter yields quantitatively, but not qualitatively. In a series of papers, Jakas and Harrison[5–7] analyzed this feature in more detail and showed in particular that it is the electronic loss of target recoil atoms rather than that of the projectile which dominates the influence of S_{el} on the sputter yield.

The situation is more severe when considering spike sputtering from metals. Here, electronic stopping according to the LS scheme would quench the entire spike contribution to sputtering, reducing considerably the simulated sputter yields and the achieved crater depths, leading to disagreement with experimental data. As a consequence, in simulations of spike sputtering, usually a lower cut-off energy, E_c, is introduced, below which $S_{el}\equiv 0$. E_c is typically chosen in the range of 5–10 eV.[8–11] If $E_c=0$ is adopted, all atomic kinetic energy is ultimately converted to electronic energy; this is clearly unphysical.

Flynn and Averback[12] were the first to consider the role of electrons in energetic-ion induced spikes. They pointed out that in a situation of strong coupling between electrons and target atoms, electrons can efficiently cool the collision cascade. Such a situation arises if the electron mean free path is smaller than the radius of the spike volume, and hence if electron-phonon coupling is strong, the target is strongly disordered, and generally at high target temperatures. Finnis *et al.*[13] and Prönnecke *et al.*[14] were among the first to introduce an algorithm for spike quenching based on electron-phonon coupling into a molecular-dynamics simulation; these authors used a frictionlike force and a stochastic Langevin approach, respectively. Previously, Caro and Victoria[15] established a modeling approach to combine the higher-velocity electronic-stopping description with the lower-velocity energy loss due to electron-phonon coupling.

In a recent study, Duffy and Rutherford[11] investigated the influence of the electronic stopping parameters on radiation damage production induced by a 10 keV primary-knock-on

atom in Fe. As a prominent result they could demonstrate that in particular the electronic stopping of low-energy (<10 eV) recoils affects the number of Frenkel pairs produced. Large values of electronic stopping quench atom motion and strongly reduce (by 50%) the number of defects. The electronic stopping parameters at higher recoil energies (>10 eV) have comparatively little effect on the number of defects produced.

In the present paper, we wish to study the consequences of the electronic loss law on spike sputtering. We shall consider a concrete system, $Au_{13} \rightarrow Au$, since here experimental data are available, and simulations have previously been performed by several groups. Our main aim will be to perform a sensitivity study; by varying the parameters describing electronic stopping systematically, we want to show which features of electronic stopping are particularly decisive for modeling spike sputtering of metals.

II. METHOD

A. Molecular-dynamics simulation

We simulate the sputtering of a Au (111) crystal by Au_{13} cluster impact at normal incidence. The total cluster energy E is varied from 10 to 500 keV, corresponding to an energy per atom between 0.77 and 38.5 keV/atom. The target crystallite contains $(0.336-1.5)\times 10^6$ atoms.

A many-body potential, which reproduces the melting temperature of Au, has been employed.[16–18] As in our previous studies,[17,18] we use energy-dissipating boundaries[19] to mimic heat transport out of the simulation crystallite. Only a single simulation was performed for each bombarding energy and electronic-stopping parameter set, since fluctuations are sufficiently small for our cluster size.[20] In fact, we calculated the fluctuations in the sputter yield for 60 keV Au_{13} cluster impact on Au, and found the standard deviation to be only around 7% of the mean value.

As a criterion to decide when an atom has been sputtered, we proceed as follows: we calculate the height of the crater rim formed at the final simulation time (100 ps). We use this value as a cut-off distance above which every particle is considered sputtered. If the simulation time is long enough (after ejection of the last particle), this procedure provides a good estimator of the sputtering yield. Recently,[21] we found a more accurate procedure, with no additional computation effort, which we also use to calculate the time evolution of the sputtering yield: we use the potential cut-off radius, $r_{\mathrm{cut}}=6.2$ Å, to define around each atom its interaction sphere. All atoms which are connected (via a chain of interaction spheres) to the bottom of the simulation crystallite, constitute the bulk target; the remaining set of atoms are the sputtered atoms. This classification of atoms into two distinct subsets is efficiently implemented using the neighbor lists which are employed anyway in the molecular-dynamics simulation.

B. Electronic stopping

1. LS scheme

Besides colliding with other atoms (nuclear stopping), moving atoms may also give part of their energy to target electrons. At the atom velocities of interest here, the stopping force (energy loss per path length traveled) is taken proportional to the atom velocity v

$$F = -\left.\frac{dE}{dx}\right|_{\mathrm{el}} = nS_{\mathrm{el}} = nkv. \tag{1}$$

Here S_{el} is the electronic stopping cross section, n is the target atom number density, and k is a constant. In an often adopted scheme due to Lindhard and Scharff[4,22] (LS), this constant is given as

$$k = k_{\mathrm{LS}} = Z_1^{1/6}\frac{Z_1 Z_2}{(Z_1^{2/3}+Z_2^{2/3})^{3/2}} 8\pi\hbar a_0. \tag{2}$$

It depends on the atomic charges of projectile and target atom Z_1 and Z_2; $\hbar$ is Planck's constant and a_0 is Bohr's radius. For our case of $Z_1=Z_2=79$, we obtain $k_{\mathrm{LS}}=0.506$ eV Å ps. Unfortunately, it is not clear how well the LS scheme describes electronic stopping at the velocities of interest to us. Experimental data for Au stopping in Au seem not to be available. From the theoretical point of view, an alternative scheme due to Firsov[23] predicts only 79% of the LS value. Besides, so-called Z_1 oscillations—related to resonant states which appear in the screening electron cloud around the projectile atom—lead to (velocity-dependent) systematic deviations from the general dependence predicted by Eq. (2).[22,24] While recent density-functional-theoretic calculations allow to determine the stopping power of atoms in a homogeneous electron liquid with considerable accuracy,[25] data for the Au-Au system are not available to us.

In order to assess the influence of electronic stopping on sputtering, we investigate the effect of different values of k. We denote this by scaling the electronic stopping by a dimensionfree parameter β, which we call the *(high-velocity) stopping coefficient*:

$$S_{\mathrm{el}} = \beta k_{\mathrm{LS}} v. \tag{3}$$

Thus, $\beta=1$ is equivalent to LS stopping, while $\beta=0$ denotes pure nuclear stopping.

Since in the present paper, the temporal aspects of stopping will be relevant, it is useful to rephrase Eq. (1) as an electronic loss power

$$-\left.\frac{dE}{dt}\right|_{\mathrm{el}} = \frac{E}{\tau}, \tag{4}$$

which defines a relaxation time τ,

$$\tau = \frac{m}{2}\frac{1}{nk}, \tag{5}$$

where m is the Au atom mass. For the system which we shall simulate in this paper, a Au atom moving in Au, the LS scheme gives values of $nk_{\mathrm{LS}}=288$ amu/ps and a relaxation time of

$$\tau_{\mathrm{LS}} = 0.34 \text{ ps}. \tag{6}$$

As a consequence, all atom motion will be quenched on a time scale $\cong 1$ ps due to electronic stopping. For non-LS values of electronic stopping, it is

$$\tau = \frac{\tau_{\mathrm{LS}}}{\beta}. \tag{7}$$

2. Slow atoms

In many simulations of ion-solid interaction, it is assumed that electronic stopping does not affect slow atoms. Often a cut-off energy, E_c, is introduced, below which stopping vanishes; E_c is typically chosen in the range of 5–10 eV.[8–11] The following reason may be given to justify why electronic stopping at low atomic kinetic energies may be small or negligible: At small atom velocities, atom-electron interaction is better described by the physics of electron-phonon interaction than by stopping.[12,13,15,26–28] Recent calculations of the electron-phonon constant in Au yield a value of $g=2.5\times10^{16}$ W/m^3 K.[29,30] These calculations take the band structure of Au into account and predict that g is rather independent of (electron) temperature up to 3000 K. The theoretical value is in satisfactory agreement with the experimental value of $(2.2\pm0.3)\times10^{16}$ W/m^3 K, obtained by pump-probe reflectivity measurements by Hohlfeld *et al.*[31]—for discussion of further experimental data see Ref. 30. A low-velocity relaxation time may be obtained from this value using

$$C_a \frac{\partial T_a}{\partial t} = -g(T_a - T_e). \tag{8}$$

For an electron temperature of $T_e=0$, and assuming the specific heat of Au as $C_a=3nk_B=2.44\times10^6$ J/m^3 K (k_B is Boltzmann's constant) one obtains the relaxation time for the atom temperature T_a as

$$\tau_{\text{e-ph}} = \frac{C_a}{g} = 98 \text{ ps}. \tag{9}$$

This value is slightly above the value of 64 ps given by Koponen,[26,27] since the recent calculations[29,30] take the full structure of the electronic density of states into account.

In order to allow for a reduction in electronic stopping at slow atom velocities, we introduce a (small) low-velocity electron-stopping parameter γ. Thus, we describe the electronic stopping cross section as

$$S_{\mathrm{el}} = \begin{cases} \beta k_{\mathrm{LS}} v, & E > E_c, \\ \gamma k_{\mathrm{LS}} v, & E < E_c, \end{cases} \tag{10}$$

where the cut-off energy E_c (corresponding to a cut-off velocity $v_c=\sqrt{2E_c/m}$) separates a faster relaxation at high atom energies from a slower relaxation at small atom energies, cf. Fig. 1.

In view of the missing detailed knowledge of S_{el} (see discussion above), we treat E_c, β, and γ as parameters in the following study. For reasons of computational convenience, we apply electronic stopping only to atoms which are below the initial target surface; in this way we attempt to exclude all sputtered particles from electronic stopping. In order to justify our simplified procedure, we recently published an investigation, in which our algorithm was compared with the results of a simulation, in which electronic stopping depends on the local density,[21] and hence some information on the atomic environment is included in the description; we found that the results of the two descriptions are in good agreement with each other.

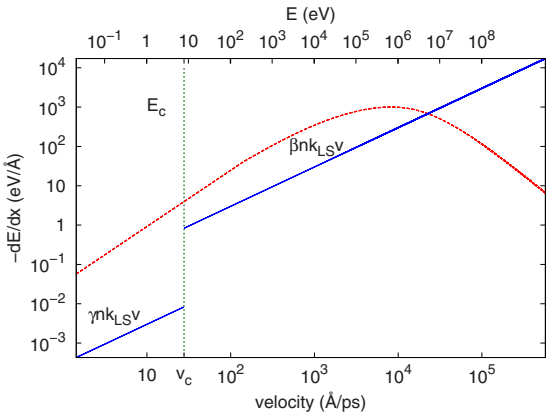

FIG. 1. (Color online) Dependence of the stopping force, $-dE/dx$, of a Au atom in Au as a function of its velocity v (bottom abscissa) and its kinetic energy E (top abscissa). Nuclear stopping (dashed) has been evaluated according to the ZBL potential (Ref. 37). Electronic stopping is assumed to be velocity proportional with two different proportionality constants, for energies above and below the cut-off energy E_c, Eq. (10). In this plot the values $\beta=1$, $\gamma=0.01$, and $E_c=7.86$ eV have been adopted.

III. RESULTS

A. Influence of high-velocity stopping coefficient β

Figure 2 assembles various data on the influence of the stopping power parameter β on the sputter behavior. We present the data for 500 keV impact energy as an exemplary case; data for lower impact energies will be summarized in Sec. III D, Fig. 8, below. In the simulations shown here, only the high-velocity stopping coefficient β has been varied; the cut-off energy was chosen as $E_c=7.86$ eV and below this energy the stopping completely vanishes, $\gamma=0$. Figure 2(a) shows how the sputter yield decreases with increasing β. For small $\beta\lesssim1$, the decrease is roughly linear, and it is

$$Y_\beta \cong (1 - 0.54\beta)Y_0, \tag{11}$$

where Y_β denotes the sputter yield with inclusion of electronic stopping and Y_0 is the sputter yield without electronic stopping. The initial slope 1/2 describes the data quite well up to $\beta\cong1$, where the sputter yield of $Y_0=41\,000$ has decreased to 20 000. For larger electronic stopping, the yield levels off.

Figure 2(b) shows the total energy given to the electronic system, E_{diss}. A considerable fraction, 50% of the impact energy for the LS value of $\beta=1$, is given to the electronic system. Figure 2(c) displays the time evolution of the energy dissipated into the electronic system. It shows that electronic stopping is active only in the first ps after projectile impact; after $t=1$ ps, no further energy is delivered into the electronic system. This is a consequence of the cut-off E_c applied: after 1 ps all Au atoms have slowed down below this

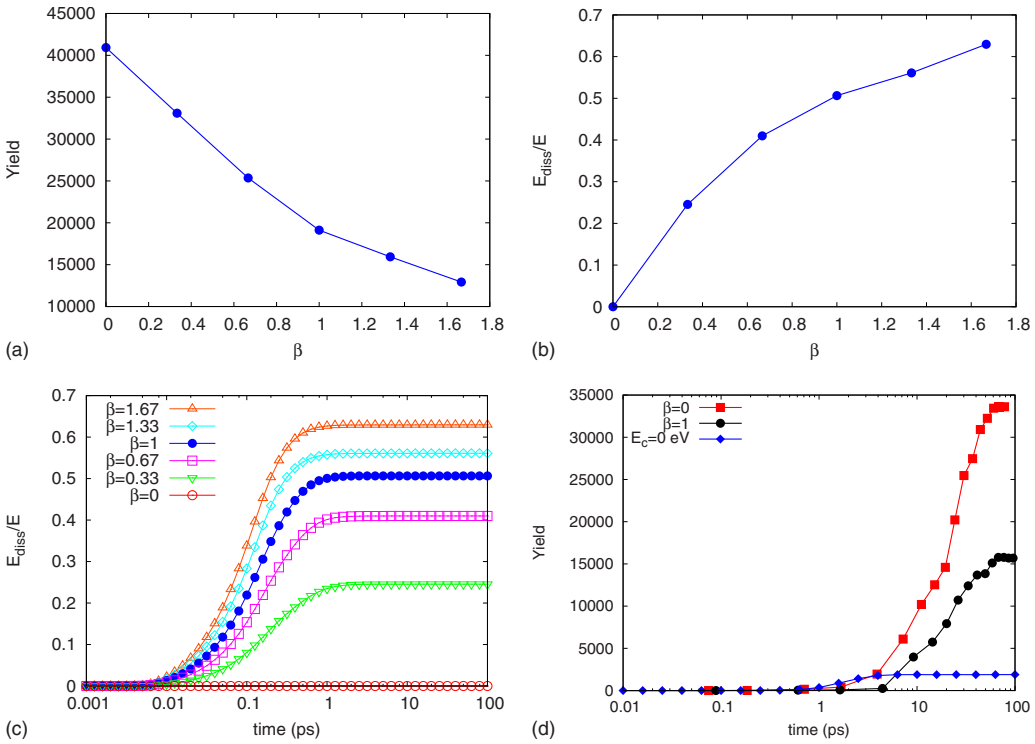

FIG. 2. (Color online) Characteristics of sputtering induced by 500 keV Au_{13} clusters on Au as a function of the high-velocity electronic-stopping coefficient β. Below the cut-off $E_c=7.86$ eV, electronic stopping vanishes, $\gamma=0$. (a) Sputter yield. (b) Energy dissipated into the electronic system, E_{diss}. (c) Time dependence of energy dissipation. (d) Temporal evolution of sputter yield for three cases: no electronic stopping ($\beta=0$), LS stopping ($\beta=1$), and LS stopping holding down to zero energy ($E_c=0$ eV).

energy and electronic stopping is not operative any longer.

In Fig. 2(d), we show the time evolution of the sputtering yield. Evidently, the sputter process takes several tens of ps until the majority of material has been ejected. However, within the first one or two ps, i.e., during the time in which electronic stopping is active, only a negligible amount of material is ejected. Thus it is understandable that electronic stopping influences the magnitude but not the temporal evolution of the sputter yield. Note that emission is retarded somewhat in the case of LS stopping with respect to the case of zero stopping. We attribute this to fluctuations in the energy deposition process rather than to the inclusion of electronic stopping, since S_{el} operates in the first ps only.

Due to this strong temporal separation of electronic energy loss and sputter events, we may hypothesize that the main effect of electronic energy loss on sputtering is the reduction in the energy available for sputtering. Denoting the sputter yield at impact energy E with inclusion of electronic stopping as $Y_\beta(E)$, and the sputter yield with $S_{\text{el}}=0$ as Y_0 consequently, we may write this hypothesis as

$$Y_\beta(E) = Y_0(E - E_{\text{diss}}). \tag{12}$$

That is, only the energy given to the atomic system, $E-E_{\text{diss}}$, is important for sputtering. Figure 3 tests this model by plotting the simulated sputter yields [Fig. 2(a)] vs $E-E_{\text{diss}}$, and compares these results with available data[18] for vanishing electronic stopping. All data nicely line up on a single curve, giving evidence in favor of the hypothesis, Eq. (12). In order to be more quantitative, we draw a linear fit line of the form

$$Y_0(E) = a\frac{E - E_{\text{th}}}{U}, \quad E > E_{\text{th}} \tag{13}$$

through the data, where $U=3.79$ eV is the cohesive energy of Au. Our fit values $a=0.246$ and $E_{\text{th}}=26.6$ keV are quite similar to the results found in Ref. 18, ($a=0.246$ and E_{th}

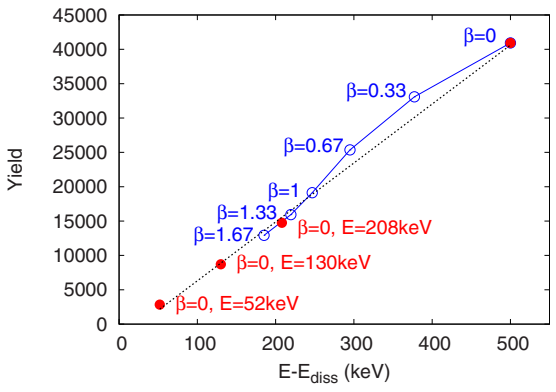

FIG. 3. (Color online) Dependence of sputter yield on the energy remaining in the atomic system, $E-E_{\text{diss}}$. Data from simulations at various impact energies E without electronic losses ($\beta=0$) (Ref. 18) and data of $E=500$ keV impacts, Fig. 2(a), with various high-velocity electronic-stopping coefficients β are combined. The dotted line gives an analytical fit, Eq. (13), to the data.

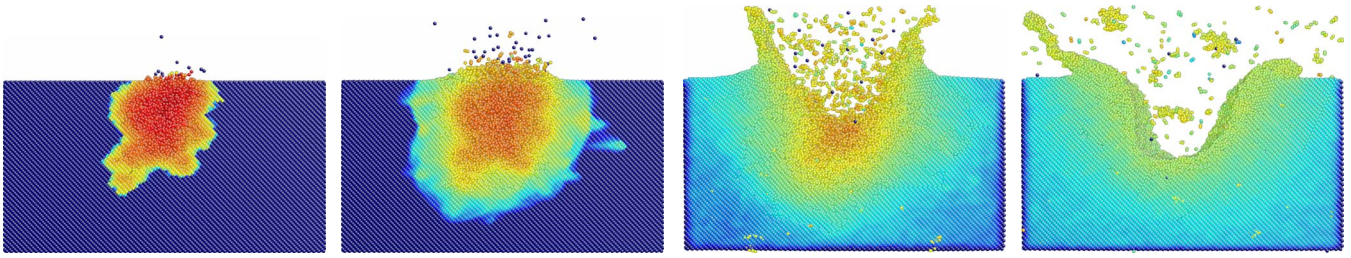

FIG. 4. (Color online) Cross-sectional view through the target Au crystallite at various times after 500 keV Au_{13} impact (Ref. 21). Electronic stopping parameters: $\beta=1$, $E_c=7.86$ eV, and $\gamma=0$. In the online version, colors denote local temperature: dark blue: 0 K, cyan: 100 K, green: 1000 K, yellow: 3000 K, orange: 10 000 K, red: above 10 000 K. Times from left to right are 0.25, 1, 10, and 50 ps.

=24.1 keV), if the results given there are linearized. In summary, it is observed that in agreement with Eq. (12), the sputter yields Y_β are well described using the predictions for Y_0, evaluated at the energy $E-E_{\mathrm{diss}}$.

Figure 4 exemplifies in the form of atomistic snapshots the processes leading to sputtering for the case of 500 keV Au_{13} impact studied here ($\beta=1$). At early times, $t\leq 1$ ps, only few atoms are sputtered; these originate in the so-called *collision-cascade* phase of sputtering[1] and are emitted individually due to the recoil momentum obtained in the collision with an energetic atom. At 10 ps, when the sputter process has reached its full activity [cf. Fig. 2(d)], Au atoms are emitted collectively from the so-called *spike*[20,32,33] volume; their emission is due to the high energy density delivered in this volume which leads to a phase explosion (gas flow) out of this volume, giving rise to abundant ejection yields. These snapshots thus display the mechanism behind the temporal evolution of the sputter yield displayed in Fig. 2(d).

B. Influence of cut-off energy E_c

Figure 5 shows the influence of the cut-off energy E_c on sputtering. Here the LS value of the high-velocity electronic stopping $\beta=1$ was chosen. Again subthreshold recoils do not suffer electronic losses, $\gamma=0$.

The effect of a small value of E_c on the sputter yield [Fig. 5(a)] is even more drastic than that of changing the electronic stopping β. In particular, when E_c is below 1.5 eV ($v_c<12$ Å/ps), the sputter yield drops to below 2300 atoms. This corresponds to a reduction by 88% from the higher cut-off energy $E_c=7.86$ eV, and of more than 94% to the case when no electronic stopping is included. However, decreasing E_c below 1.5 eV does not influence the sputter yields any more; as we shall show in the snapshots of Fig. 6 below, this is due to the fact that sputtering is then predominantly due to collision-cascade events, for which the atom motion below the cohesive energy is of little importance.

The dissipated energies [Fig. 5(b)] monotonously increase with lowering E_c. We plot these data vs v_c rather than E_c, in order to demonstrate the apparent linear dependence of E_{diss} on v_c. When $E_c=0$, i.e., all moving atoms suffer electronic stopping, $E_{\mathrm{diss}}=480$ keV; i.e., only 4% of the impact energy remains in atomic motion; this is the energy of atoms which have left the target. The transition toward this extreme case is obviously quite soft; setting the cut-off at $E_c=0.31$ eV—in a thermalized atom ensemble, this corresponds to a temperature of above 2000 K—the losses still amount to >85%.

Figure 5(c) demonstrates a clear influence of E_c on the time structure of the energy dissipated into the electronic system; note that the high-velocity stopping coefficient β showed no such influence [Fig. 3(c)]. While the dissipation ceases at around 0.5 ps for the highest value studied ($E_c=7.86$ eV), dissipation proceeds until 5 ps, and even beyond, for the two smallest values of the cut-off energy (0.31 and 0 eV). Since this time is well in the spike sputter phase, we have to expect that not only the collision-cascade phase of sputtering, but also the spike phase is affected by these small values of the cut-off energy. Indeed, as was shown in Fig. 2(d), sputtering ceases quickly for $E_c=0$ eV; the collision spike which was visible in the snapshots of Fig. 4 is quickly quenched such that the gas-flow mechanism of sputtering cannot become operative.

Figure 6 shows snapshots which prove this view. Evidently, at the two earliest times, $t=0.1$ and 0.4 ps, the sys-

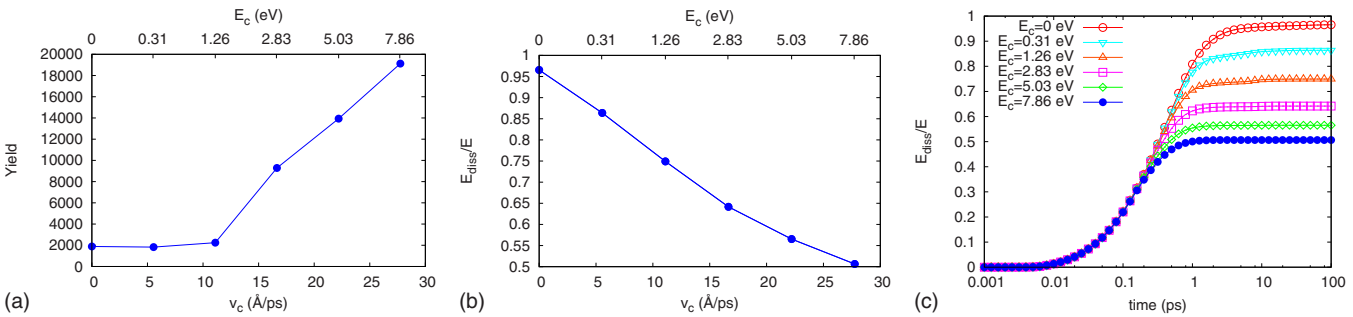

FIG. 5. (Color online) Analogous to Fig. 2. Here the cut-off velocity v_c, below which electronic stopping vanishes, $\gamma=0$, has been varied, while the high-velocity electronic-stopping coefficient β is fixed at $\beta=1$.

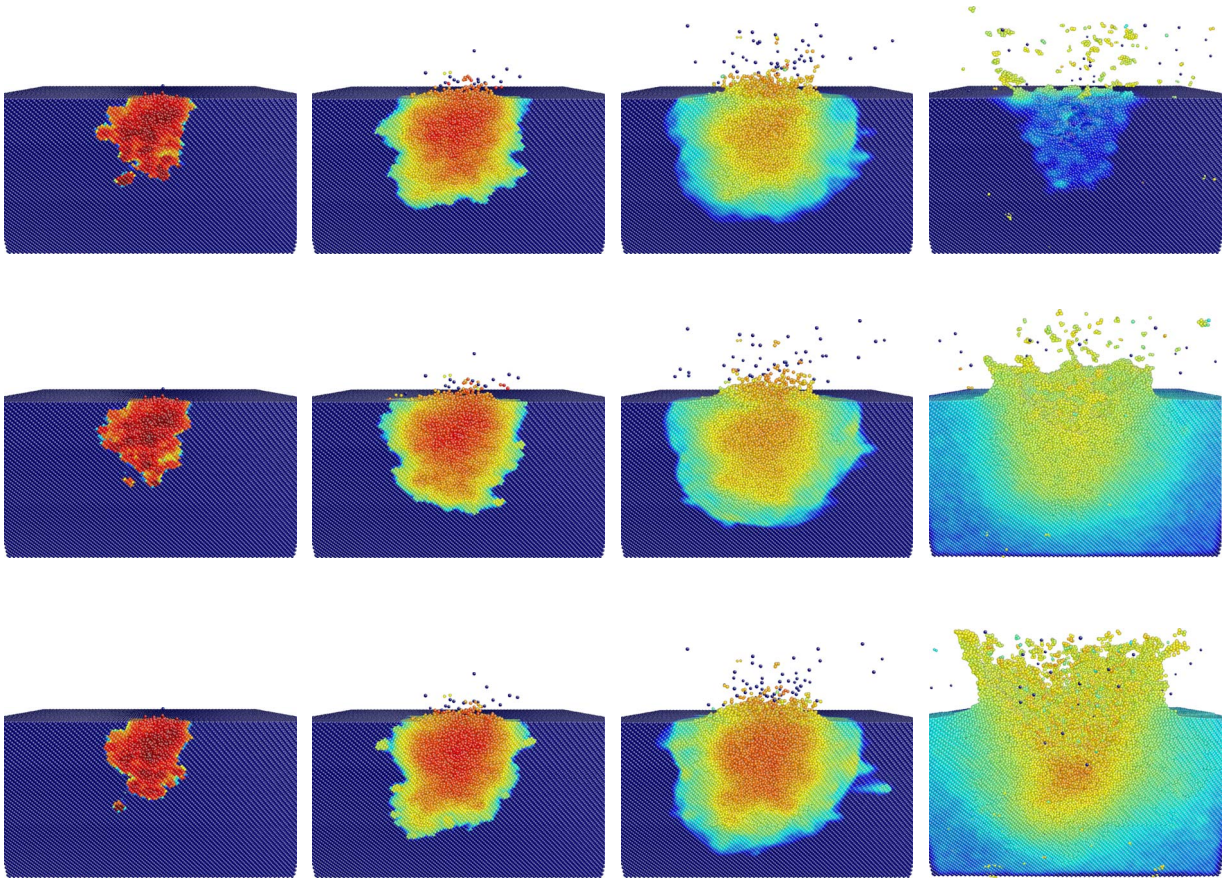

FIG. 6. (Color online) Perspective view of the target Au crystallite, cut through the center of the cluster impact point, at various times t after 500 keV Au_{13} impact. Electronic stopping parameters: $\beta=1$, E_c as indicated, $\gamma=0$. Color code as in Fig. 4. Top row: $E_c=0$ eV, middle row: $E_c=1.26$ eV, bottom row: $E_c=7.86$ eV. Columns from left to right are at times of 0.1, 0.4, 1.0, and 10 ps.

tems develop quite similarly for the three cut-off energies displayed. The small deviations visible are due to fluctuations in the energy deposition in the collision cascade phase of projectile slowing down. However, already at 1 ps, it becomes clear that energy is still contained in the spike volume for the high cut-off energy, while energy has been dissipated out of this volume for the two smaller cut-off energies; however, the expansion of the spike volume toward the surface, which has been necessitated by the high thermoelastic pressure induced by the high energy density delivered in this volume, and the concomitant beginning sputtering are visible in all three cases. At 10 ps, however, the consequences of the strong spike quenching for $E_c=0$ and 1.26 eV become clear: while emission is still active from the spike volume (in the snapshot still energy gradients are visible, which are connected to pressure gradients driving the expansion), the spike has been quenched for the case of $E_c=0$ eV and emission has terminated; the case of $E_c=1.26$ eV is intermediate.

C. Influence of low-velocity stopping coefficient γ

Figure 7 shows the effect of including a small electron stopping γ below the cut-off energy of $E_c=7.86$ eV; in this series of simulations, the value of the high-velocity stopping

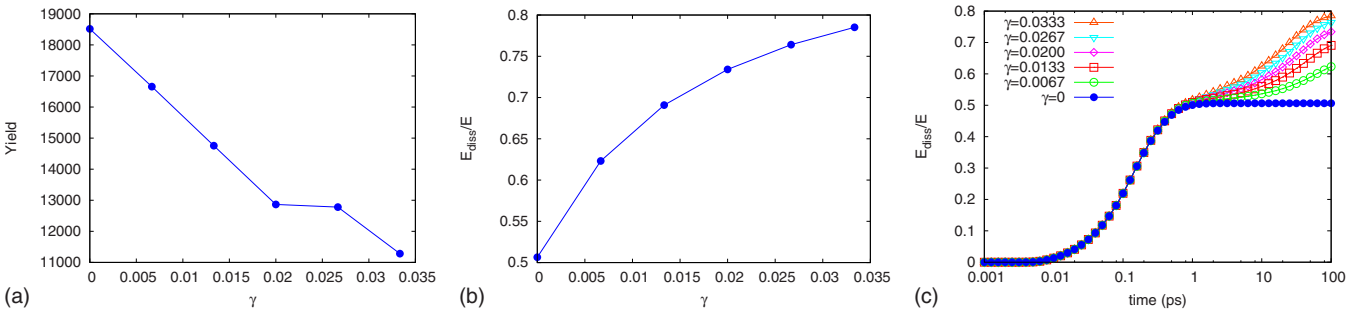

FIG. 7. (Color online) Analogous to Figs. 2 and 5. Here the low-velocity electronic-stopping coefficient γ has been varied, while the high-velocity electronic-stopping coefficient $\beta=1$ and the cut-off energy $E_c=7.86$ eV are fixed.

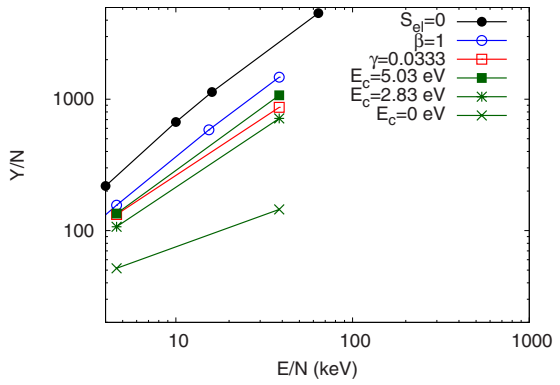

FIG. 8. (Color online) Dependence of the sputter yield per projectile atom, Y/N, on the impact energies per atom, E/N for various electronic stopping parameters. Data for $S_{el}=0$ neglect all electronic stopping (Ref. 18). Data for a given value of the cut-off energy E_c assume LS stopping ($\beta=1$) above that energy, and vanishing stopping ($\gamma=0$) below it. The data denoted by $\beta=1$ assumes $E_c=7.86$ eV ($\gamma=0$) and refers to the simulation results plotted in Fig. 4. The same values of E_c and $\beta=1$ apply to the data denoted by $\gamma=0.033$; in addition, low-velocity stopping has been included with this value of γ.

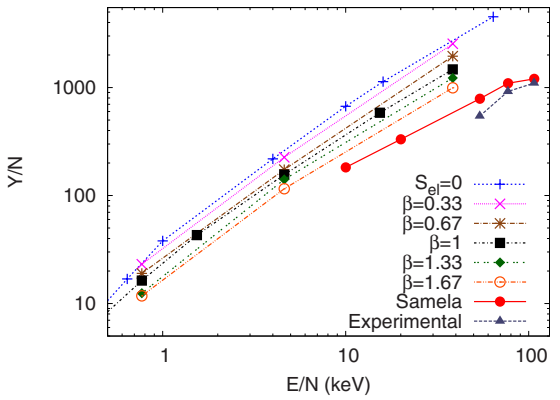

FIG. 9. (Color online) Synopsis of sputter yields per projectile atom, Y/N, obtained for Au_{13} impact into Au for various impact energies per atom, E/N. Experimental data taken from Ref. 34. All other data obtained by simulation. Data by Samela *et al.* (Ref. 35) have been obtained using the CEM potential (Ref. 38) and for electronic stopping described by the parameters $\gamma=0$, $\beta=1$, and $E_c=5$ eV. Data for $S_{el}=0$ by Zimmermann *et al.* (Ref. 18) have been obtained by the Colla (Refs. 16–18) potential. All other data are results of the simulations presented here using the Colla potential, and including high-velocity stopping (β as indicated) above a cut-off energy of $E_c=7.86$ eV, and no low-velocity stopping, $\gamma=0$.

coefficient has been kept constant at $\beta=1$. Figure 7(a) demonstrates a definite, albeit small, influence on the sputter yield. We see that, even though the effect is operative over a time scale of several tens of ps, over which sputtering occurs, the overall effect is moderate; the sputter yield decreases from 18500 to around 11300 at the most, a 39% effect. The influence of the low-velocity stopping coefficient on the sputter yield is monotonic with the exception of the simulation for $\gamma=0.027$; here a fluctuation in the emission process (ejection of a large cluster) influenced the sputter yield. The effect of γ on the dissipated energy is, however, quite monotonic; besides the 50% of the impact energy which are dissipated to the electronic system within the first ps due to high-velocity stopping (cf. Fig. 2), low-velocity stopping removes a further amount of up to 30% of the impact energy out of the atomic system. Figure 7(c) proves that the dissipation process is not yet over at the end of the simulation time (100 ps) but will continue, until all atomic energy (with the exception of that of sputtered particles) has been dissipated. However, this will happen long after sputtering has ceased and is hence of no influence here.

D. Dependence on impact energy

In addition to the simulations with 500 keV impact energy, we performed a number of simulations with 60 keV and a few with 10 keV impact energy. We collect these results in Fig. 8. The data at lower impact energy show the same systematic dependence on the electronic-stopping parameters as the 500 keV results discussed up to now. The strong influence of β and the dominant role of E_c show up clearly in this presentation, while the role of γ is minor.

However, this plot allows to observe that the influence of the electronic-stopping parameters diminishes with decreasing bombarding energy. As a consequence the slope of the curves in the double-logarithmic plot, Fig. 8,—i.e., the local power-law behavior, $Y \propto E^m$—flattens. In the restricted range of simulations presented, the slope changes from $m=1.0\ldots1.1$ for no stopping or LS stopping, over $m=0.9\ldots1.0$ for $\gamma=0.033$ and $E_c=2.83$ or 5.03 eV to $m=0.5$ for $E_c=0$. Note that the simple analytical sputter-yield law, Eq. (13), predicts sputtering to cease at $E=E_{th}=26.6$ keV, i.e., at $E/N \cong 1.8$ keV; our smaller impact energy is already in the vicinity of this energy. Here the spike contribution to sputtering becomes small and mainly collision cascades contribute to sputtering; this latter process is fast (<1 ps), and hence electronic stopping has less time to suck energy out of the atomic system. This explains why the influence of the electronic-stopping parameters becomes smaller at low energies.

We conclude that an increased value of $\beta>0$ reduces the yield, but does not change the slope. This makes sense since the high-velocity stopping β only acts in the first ps, when there is still no (or only negligible) sputtering. The yield reduction itself is monotonic in β and can be read off Fig. 2(a). However, low-velocity stopping $\gamma>0$ does change the slope—this means it influences more the 500 keV data than the 60 keV data. An even more pronounced effect is seen for small values of E_c, which strongly reduces the slope. In summary, as soon as electronic losses happen *during* the spike phase, the linearity in $Y(E)$ is lost.

E. Comparison to experimental data

Sputtering of Au by Au_{13} impact has been measured at impact energies between 1–2 MeV,[34] i.e., only slightly above the impact energies of our simulations. Besides these data, three sets of simulation data are included in Fig. 9. The data by Samela *et al.*[35] are presumably the best data available; they assume LS electronic stopping ($\beta=1$) above a cut-off

energy $E_c=5$ eV, and $\gamma=0$ otherwise. The simulation lasted 100 ps; the dynamics of the sputtered material was continued beyond 2 μs, in order to take fragmentation and back deposition of sputtered clusters on the surface into account. The interatomic potential employed in that study is known to describe solid Au and also small Au clusters well; the only disadvantage is the rather high melting temperature (30% higher than experiment) predicted by this potential. Since the sputter yield in the spike regime is known to depend sensitively on the melting temperature of the potential,[17] this introduces a possible source of error of roughly 30% to these data. Furthermore we included the simulation results by Zimmermann *et al.*[18] with $\beta=0$ and the present simulation results with $\beta=1$. The deviation between the present simulation results and those of Samela *et al.* are due to (i) the different interatomic potential employed; this feature demonstrates the influence of the interatomic interaction potential on spike sputtering; (ii) the different simulation time (estimated to affect the result by 30%).

We also include the simulation data obtained with $E_c=0$, assuming the high-velocity LS stopping to be valid down to vanishing atomic kinetic energies; as demonstrated above, this gives only the collision cascade contribution to sputtering but quenches the spike contribution. Clearly these data underestimate strongly the experimental sputter yields. We hence conclude that the experimental sputter data contain a strong and even dominant contribution of spike sputtering. This comparison thus gives evidence that it is unrealistic to assume LS stopping to hold down to zero atom energies.

IV. CONCLUSIONS

We investigated the effect of electronic stopping on the sputtering from metallic targets in the spike regime. As a concrete example, we studied the sputtering of Au induced by Au_{13} clusters with energies of 500 keV and below. We conclude from our results that the exact nature of the electron-atom coupling for low-energy (<10 eV, say) atom motion in solids appears not to be clearly resolved. While a velocity-proportional frictionlike stopping force is always assumed, the exact value of the proportionality factor is being debated. As a rule, it is assumed that at small atom energies, this proportionality factor is considerably smaller than at high energies. We performed model simulations to quantify the effect of various electronic loss laws on the sputter yield.

In many, if not all, simulational studies, electronic stopping is included only for atom energies above a cut-off energy E_c, where E_c is chosen in the range of 5–10 eV. In this case, electronic stopping only affects the early collision-cascade phase and the spike which is responsible for the majority of sputtering is not affected. Even though the yield reduction due to the inclusion of electronic stopping may be sizable (up to 50%), the effect of the electronic stopping can be understood in a simple model: The sputter yield induced by an impact with energy E, in which the energy E_{diss} is dissipated to the electronic system, is identical to that with an energy $E-E_{\mathrm{diss}}$, when electronic stopping is ignored.

The effects of electronic stopping become more pronounced, when the cut-off energy E_c is lowered. If E_c is smaller than roughly one half the cohesive energy of the target, the spike is effectively quenched and does not contribute to sputtering any longer. Still, the collision-cascade phase—a few ps after impact—contributes to sputtering; the yield is only on the order of 10% or less of the sputter yield without electronic stopping. Then, more than 90% of the impact energy are given to the electronic system of the target.

It has been debated whether low-velocity atom stopping is governed by the same stopping law as at higher energies. In particular, optical experiments give evidence for an electron-atom relaxation time which may be two orders of magnitude smaller than the relaxation time governing ion slowing down. We show that due to the long time scales over which sputtering proceeds even such a small electron-atom coupling may lead to energy dissipation in the order of 30% and a comparable decrease of the sputter yield.

Our results demonstrate that a careful modeling of the electronic stopping is crucial for obtaining a detailed quantitative understanding of spike sputtering. Even the qualitative nature of the sputtering process changes, i.e., spikes may be entirely quenched if slow atoms suffer a strong electronic energy loss. A detailed modeling will require to include the space and time dependent temperature of the electronic system. In the present paper, as in most other simulations, electrons are modeled only as a heat sink. When a finite electron temperature is taken into account, the electron-atom friction will be reduced. The small stopping coefficient γ adopted in our study may be viewed as a simple-minded modeling approach to incorporate in an effective way such a reduced friction coefficient.

We note that the electron-phonon coupling will depend on the (thermodynamic) local state of material; it may be different in the gas, liquid, and crystalline phases. In more detail it will depend on the local temperature and density. We note that Wucher *et al.*[36] have implemented a numerical scheme to solve the coupled electron and atom dynamics in ion bombarded solids. We note two major results of that work: (i) the computational algorithm is extremely slow, and at the present time not yet suited to treat the spike sputtering phenomena as in the present work (due to the longer space and time scales occurring here); (ii) several of the important materials parameters describing the electron-atom coupling (such as the electron-phonon coupling and the electron mean free path) are not available in their full dependence on atom and electron temperature, atom density, and local atomic disorder.

Experimental data appear to be modeled reasonably well using the conventional coupling scheme, i.e., switching electronic stopping entirely off below a cut-off energy. In particular, this agreement gives evidence that it is unrealistic to assume electronic stopping to be operative with the same high stopping constant as for higher energies. A drop of the stopping constant by 2 orders of magnitude is consistent with the experimental data.

ACKNOWLEDGMENTS

The authors acknowledge support by the Deutsche Forschungsgemeinschaft via the Graduiertenkolleg 814.

*urbassek@rhrk.uni-kl.de; http://www.physik.uni-kl.de/urbassek/

[1] *Sputtering by Particle Bombardment I*, edited by R. Behrisch (Springer, Berlin, 1981).
[2] *Sputtering by Particle Bombardment*, Topics Appl. Physics Vol. 110, edited by R. Behrisch and W. Eckstein (Springer, Berlin, 2007).
[3] P. Sigmund, Appl. Phys. Lett. **25**, 169 (1974); **27**, 52 (1975).
[4] J. Lindhard and M. Scharff, Phys. Rev. **124**, 128 (1961).
[5] M. M. Jakas and D. E. Harrison, Jr., Phys. Rev. B **30**, 3573 (1984).
[6] M. M. Jakas and D. E. Harrison, Jr., Phys. Rev. B **32**, 2752 (1985).
[7] D. E. Harrison, Jr. and M. M. Jakas, Nucl. Instrum. Methods Phys. Res. B **15**, 25 (1986).
[8] Y. Zhong, K. Nordlund, M. Ghaly, and R. S. Averback, Phys. Rev. B **58**, 2361 (1998).
[9] E. E. Zhurkin and A. S. Kolesnikov, Nucl. Instrum. Methods Phys. Res. B **202**, 269 (2003).
[10] J. Samela, J. Kotakoski, K. Nordlund, and J. Keinonen, Nucl. Instrum. Methods Phys. Res. B **239**, 331 (2005).
[11] D. M. Duffy and A. M. Rutherford, J. Phys.: Condens. Matter **19**, 016207 (2007).
[12] C. P. Flynn and R. S. Averback, Phys. Rev. B **38**, 7118 (1988).
[13] M. W. Finnis, P. Agnew, and A. J. E. Foreman, Phys. Rev. B **44**, 567 (1991).
[14] S. Prönnecke, A. Caro, M. Victoria, T. Diaz de la Rubia, and M. W. Guinan, J. Mater. Res. **6**, 483 (1991).
[15] A. Caro and M. Victoria, Phys. Rev. A **40**, 2287 (1989).
[16] T. J. Colla and H. M. Urbassek, Nucl. Instrum. Methods Phys. Res. B **164-165**, 687 (2000).
[17] S. Zimmermann and H. M. Urbassek, Nucl. Instrum. Methods Phys. Res. B **228**, 75 (2005).
[18] S. Zimmermann and H. M. Urbassek, Nucl. Instrum. Methods Phys. Res. B **255**, 208 (2007).
[19] J. R. Beeler, Jr., *Radiation Effects Computer Experiments* (North-Holland, Amsterdam, 1983).
[20] T. J. Colla, R. Aderjan, R. Kissel, and H. M. Urbassek, Phys. Rev. B **62**, 8487 (2000).
[21] L. Sandoval and H. M. Urbassek, Nucl. Instrum. Methods Phys. Res. B (to be published).
[22] P. Sigmund, R. Bimbot, H. Geissel, H. Paul, and A. Schinner, J. ICRU **5**, 1 (2005).
[23] O. B. Firsov, Sov. Phys. JETP **36**, 1076 (1959).
[24] P. M. Echenique and M. E. Uranga, in *Interaction of Charged Particles with Solids and Surfaces*, NATO Advanced Studies Institute, Series B: Physics, edited by A. Gras-Martí, H. M. Urbassek, N. R. Arista, and F. Flores (Plenum Press, New York, 1991), Vol. 271, p. 39.
[25] V. U. Nazarov, J. M. Pitarke, Y. Takada, G. Vignale, and Y.-C. Chang, Phys. Rev. B **76**, 205103 (2007).
[26] I. Koponen, J. Appl. Phys. **72**, 1194 (1992).
[27] I. Koponen, Phys. Rev. B **47**, 14011 (1993).
[28] R. S. Averback and T. Diaz de la Rubia, in *Solid State Physics*, edited by H. Ehrenreich and F. Spaepen (Academic Press, Boston, 1998), Vol. 51, p. 281.
[29] Z. Lin and L. V. Zhigilei, Proc. SPIE **6261**, 62610U (2006).
[30] Z. Lin, L. V. Zhigilei, and V. Celli, Phys. Rev. B **77**, 075133 (2008).
[31] J. Hohlfeld, S.-S. Wellershoff, J. Güdde, U. Conrad, V. Jähnke, and E. Matthias, Chem. Phys. **251**, 237 (2000).
[32] H. M. Urbassek and J. Michl, Nucl. Instrum. Methods Phys. Res. B **22**, 480 (1987).
[33] H. M. Urbassek, in *Handbook of Surface Science*, edited by E. Hasselbrink and B. I. Lundqvist (Elsevier, Amsterdam, 2008), Vol. 3, Chap. 17, pp. 871–913.
[34] S. Bouneau, A. Brunelle, S. Della-Negra, J. Depauw, D. Jacquet, Y. LeBeyec, M. Pautrat, M. Fallavier, J. C. Poizat, and H. H. Andersen, Phys. Rev. B **65**, 144106 (2002).
[35] J. Samela and K. Nordlund, Phys. Rev. B **76**, 125434 (2007).
[36] A. Duvenbeck, O. Weingart, V. Buss, and A. Wucher, N. J. Phys. **9**, 38 (2007).
[37] J. F. Ziegler, J. P. Biersack, and U. Littmark, *The Stopping and Range of Ions in Solids* (Pergamon, New York, 1985).
[38] C. L. Kelchner, D. M. Halstead, L. S. Perkins, N. M. Wallace, and A. E. DePristo, Surf. Sci. **310**, 425 (1994).